Computers and Concrete, *Vol. 22, No. 3 (2018) 291-303*
DOI: https://doi.org/10.12989/cac.2018.22.3.291

Experimental study on the dynamic behavior of pervious concrete for permeable pavement

Jingwu Bu[1,2a], Xudong Chen[*3], Saisai Liu[3b], Shengtao Li[3c] and Nan Shen[3d]

[1]School of Hydraulic Energy and Power Engineering, Yangzhou University, Yangzhou, 225009, PR China
[2]State Key Laboratory of Hydrology-Water Resources and Hydraulic Engineering, Hohai University, Nanjing, 210098, PR China
[3]College of Civil and Transportation Engineering, Hohai University, Nanjing, 210098, PR China

(Received February 21, 2017, Revised August 30, 2018, Accepted September 11, 2018)

Abstract. As the concept of "sponge city" is proposed, the pervious concrete for permeable pavement has been widely used in pavement construction. This paper aims at investigating the dynamic behavior and energy evolution of pervious concrete under impact loading. The dynamic compression and split tests are performed on pervious concrete by using split Hopkinson pressure bar equipment. The failure criterion on the basis of incubation time concept is used to analyze the dynamic failure. It is demonstrated that the pervious concrete is of a strain rate sensitive material. Under high strain rate loading, the dynamic strength increases while the time to failure approximately decreases linearly as the strain rate increases. The predicted dynamic compressive and split tensile strengths based on the failure criterion are in accordance with the experimental results. The total damage energy is found to increase with the increasing of strain rate, which means that more energy is needed to produce irreversible damage as loading rate increases. The fractal dimensions are observed increases with the increasing of impact loading rate.

Keywords: pervious concrete; dynamic behavior; incubation time concept; energy evolution; fragments

1. Introduction

Pervious concrete was developed as an environmentally friendly material in recent years (ACI 522R 2010, Volder *et al*. 2009, Novom *et al*. 2013). It is a special cementitious material composed of coarse aggregates and no fine aggregate, and cemented by thin layer cement paste. Because of the special composition of pervious concrete, it incorporates high number of pores which makes the mechanical behavior different from that of normal concrete. For this reason, it is generally being used in constructions that require higher permeability, better noise absorption and thermal insulation. As the concept of "sponge city" is proposed, the pervious concrete has been widely used in pavement construction. Recently, pervious concrete have seen renewed interest in this type of pavements due to its ability to allow water to flow through itself to recharge groundwater and minimize storm water runoff (Monters 2006, Sumanasooriya and Neithalath 2011). However, as higher porosity is required, little or no fine aggregate is added to the mixture. So coarse aggregates in the mixtures are bonded together with very thin cement paste layers rather than embedded in cement paste as in normal concrete (Torres *et al*. 2015, Zhong and Wille 2016, Kuo *et al*. 2013, Rehder *et al*. 2013, Joshaghani *et al*. 2015.).

Pervious concrete pavement is commonly subjected to dynamic loading. Therefore, it is essential to conduct investigations on the dynamic behavior of pervious concrete. Because of the high intentional air void in the structure, the static strength of pervious concrete is smaller than that of normal concrete (Lian *et al*. 2011, Li and Aubertin 2003). Its dynamic behavior under impact loading is considerably different from that of normal concrete (Ozbek *et al*. 2013). Under dynamic compressive loading, fragmentations are formed as the coalescence of microcracks in pervious concrete, so the fragments size is dependent on the distribution of microcracks. In pervious concrete, as the cement paste embedded in the space of coarse aggregates is very thin, the fracture pattern is mainly affected by the geometry of coarse aggregates (Lian and Zhuge 2010). Therefore, the ultimate crack pattern and strength of pervious concrete are different from those of normal concrete. The stress in statics is commonly considered as a constant material property, while the stress in dynamics increases with the loading rate, and the enhancement is defined as the dynamic increase factor (DIF). Many researches have studied the dynamic strength of concrete at high strain rates (Zielinski *et al*. 1981, Rossi *et al*. 1994, Brara and Klepaczko 2006, Yan and Lin 2006, Cadoni *et al*. 2007, Hao *et al*. 2009, Erzar and Forquin 2010, De Andrade Silva *et al*. 2011, Zhu *et al*. 2011, Chen

*Corresponding author, Professor
E-mail: cxdong1985@hotmail.com
[a]Lecturer
E-mail: bujingwu2008@163.com
[b]Undergraduate Student
E-mail: ssmoondream@163.com
[c]Undergraduate Student
E-mail: 13707366178@163.com
[d]Undergraduate Student
E-mail: shennan19970822248@163.com

http://www.techno-press.org/?journal=cac&subpage=8
ISSN: 1598-8198 (Print), 1598-818X (Online)

et al. 2014, Chen *et al*. 2015, Chen *et al*. 2016a, Tian *et al*. 2016, Chen *et al*. 2017). Review on the above literatures, it can be concluded that the dynamic strength of concrete increases with an increase of strain rate. It has also been discovered that concrete material is more sensitive to strain rate with higher moisture content (Ross *et al.* 1996), smaller maximum aggregate size (Cadoni *et al*. 2001) and higher cement content (Glinicki 1993). Unfortunately, there exists a very limited test data about the dynamic behavior of pervious concrete (Ozbek *et al*. 2013, Weerheijm 2016). The existing literatures are focused on the dynamic strength while do not consider the failure time and the growth of dynamic stress and the relation between them. There is at least an important reason why the dynamic tests are performed on the pervious concrete. Pervious concrete as an environmentally friendly material have been used in pavement, which is vulnerable to impact loading, the dynamic behavior of pervious concrete is necessary.

Various experimental devices can be used to carry out dynamic test on concrete-like material at various strain rates. Bending test on concrete beams have been carried out, at loading rate of 0.1 mm /s to10 mm/s, by using a hydraulic servo-controlled testing system (Xiao *et al.* 2017). Strain rates of 10^{-1} s^{-1} can be reached in concrete performed by drop weight (Banthia *et al*. 1987). Split Hopkinson pressure bar (SHPB) equipment has been commonly used to investigate the dynamic behavior of quasi-brittle materials like rock and concrete (Li *et al*. 2017, Fu *et al.* 2017). In this paper, dynamic tests are performed on pervious concrete specimens by using the SHPB equipment. Besides, the energy evolution of pervious concrete specimen under dynamic loading is studied. In the dynamic experiments, the failure patterns are also monitored by sieving mesh and the fragments are analyzed in terms of their sizes based on the fractal theory.

2. Materials and test methods

2.1 Samples preparation

The mix proportions by mass of pervious concrete are listed in Table 1. Ordinary Portland cement and mineral powder are used as the binding material. Basalt gravel with maximum size of 10 mm is used as the coarse aggregate. Tap water in the laboratory is used. Additionally, the polycarboxylate superplasticizer is used in the concrete mixes to increase the workability.

Both static and dynamic tests are performed on the pervious concrete specimens in this paper. The cylindrical specimens with diameter of 74 mm and height of 148 mm are used for the static uniaxial compression test. The disc samples with diameter of 74 mm and thickness of 37 mm are used to perform the dynamic compression and static/dynamic split tensile tests.

Table 1 The dosage of each material in unit volume pervious concrete (kg/m^3)

Water	Cement	Mineral powder	Aggregate	Water reducer
93	334.75	33.47	1425	1.485

(a) Static compression test (b) Split tensile test

Fig. 1 The failure modes of pervious concrete specimens under static loading

2.2 Static test

Static compression and split tensile tests are carried out by using the electric hydraulic material testing machine. Three samples are used for each case to reduce the discrete error. According to the advised method from ISRM, the static test is controlled by the loading rate of 0.1 kN/s. The static compressive strength is the loading capacity divided by the sectional area. The split tensile strength is calculated according to the following formula

$$\sigma_t = \frac{2P}{\pi DL} \tag{1}$$

in which, σ_t is the split tensile strength (MPa), P is the maximum load (kN), D is the diameter of specimen (mm), and L is the thickness of disc sample (mm).

According to the experimental results, the average static uniaxial compression strength and split tensile strength of pervious concrete are 12.03 MPa and 1.66 MPa, respectively. The failure modes of pervious concrete samples subjected to loading are shown in Fig. 1. The crush with vertical fractures is observed in cylindrical specimens under static compressive loading. In the static split tensile test, the Brazilian disc specimens are split into two halves.

2.3 Dynamic test

The dynamic compression and split tensile tests are carried out on the pervious concrete by using the SHPB equipment with the diameter of 74 mm. The dynamic compression test is carried out using the classical Kolsky method. The dynamic split tensile test is performed on the Brazilian disc specimens. The loading modes of dynamic tests are shown in Fig. 2.

The SHPB equipment is composed of the power system, striker, an input and output bar with lengths of 3200 mm and 1800 mm, respectively. The striker is fired using compressed nitrogen gas with set pressure. The striker has an initial velocity when it is fired. The compression wave is induced in the incident bar and transmitted into the specimen. At the same time, part of the compression wave is reflected to the incident bar and the rest is transmitted to the transmitted bar. The incident, reflected and transmitted

(a) Compressive loading

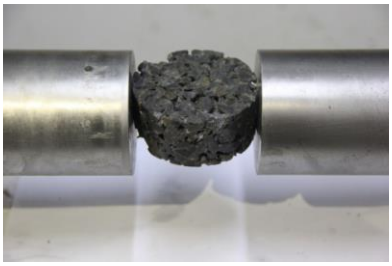

(b) Split tensile test

Fig. 2 The dynamic tests

strain waves are recorded by the strain gauges pasted to the Hopkinson pressure bars. Assuming that the energy lost in the testing system is neglected, the strain waves in the incident and transmitted bars satisfy the following formula

$$\varepsilon^{\mathrm{I}}(t)+\varepsilon^{\mathrm{R}}(t)=\varepsilon^{\mathrm{T}}(t) \tag{2}$$

in which, $\varepsilon^{\mathrm{I}}(t)$ is the incident strain, $\varepsilon^{\mathrm{R}}(t)$ is the reflected strain and $\varepsilon^{\mathrm{T}}(t)$ is the transmitted strain.

In the dynamic compression test, the dynamic compressive strength σ^{compr}, strain σ^{compr} and strain rate $\dot{\varepsilon}^{\mathrm{compr}}$ of concrete can be calculated based on the three-wave method expressed as the following formulas

$$\left.\begin{aligned} \sigma^{\mathrm{compr}}(t) &= \frac{EQ}{Q_{\mathrm{s}}}\varepsilon^{\mathrm{T}}(t) \\ \varepsilon^{\mathrm{compr}}(t) &= -\frac{2c}{L_{\mathrm{s}}}\int_0^t \varepsilon^{\mathrm{R}}(t)dt \\ \dot{\varepsilon}^{\mathrm{compr}}(t) &= -\frac{2c}{L_{\mathrm{s}}}\varepsilon^{\mathrm{R}}(t) \end{aligned}\right\} \tag{3}$$

in which, σ^{compr} is the dynamic compressive strength (MPa), σ^{compr} is the dynamic compressive strain, $\dot{\varepsilon}^{\mathrm{compr}}$ is the dynamic compressive strain rate (s^{-1}), E is the dynamic elastic modulus (GPa), Q is the diameter of the SHPB (mm), and Q_{s} is the diameter of the Brazilian disc sample (mm). In this test, both the diameters of the SHPB and Brazilian disc sample are 74 mm. The axial velocity c of strain wave along with the SHPB is 5100 m/s. The length of specimen L_{s} is 37 mm.

In the dynamic split tensile test, the time-history tensile stress of pervious concrete can be calculated by using the Eq. (4)

$$\sigma^{\mathrm{ts}}(t)=\frac{2EQ\varepsilon^{\mathrm{T}}(t)}{\pi L_{\mathrm{s}}D_{\mathrm{s}}} \tag{4}$$

in which, the diameter D_{s} of Brazilian disc specimen is 74 mm.

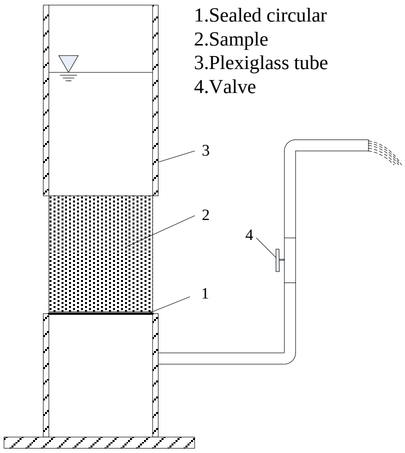

Fig. 3 Diagrammatic of the measurement of permeability of pervious concrete

In this paper, the dynamic compression test on pervious concrete is performed by using four various air pressures of 0.15 MPa, 0.2 MPa, 0.25 MPa and 0.3 MPa. And three air pressures of 0.15 MPa, 0.25 MPa and 0.35 MPa are used in the dynamic split tensile test. To reduce experimental error, three specimens are tested at one air pressure.

2.4 Porosity and permeability tests

The majority of pores in pervious concrete are formed by the spaces between coarse aggregates. In the complex microstructure of pervious concrete, the size of pores is commonly from the nano-scale to the macro-scale. According to the measurement method of total porosity proposed by Shen *et al*. (2013), the total porosity of pervious concrete can be expressed by the following formula

$$p=\left(1-\frac{\rho_{\mathrm{s}}}{\rho_{\mathrm{t}}}\right)\times 100\% \tag{5}$$

in which, p is the total porosity, ρ_s and ρ_t are the bulk density and theoretical density of the pervious concrete sample, respectively.

The tested total porosity of pervious concrete used in this test is 13%.

With the recommendation of ACI 522R (2010), the water permeability coefficient of pervious concrete was measured using the constant head method with equipment shown in Fig. 3. To prevent flow between sample and surface of measuring cylinder, the cylindrical sample was wrapped by plexiglass tube and tightened by circular clamps. The water permeability coefficient can be calculated according to the Darcy's law expressed by the following formula

$$k=\frac{QL}{HAt} \tag{6}$$

in which, k is the water permeability coefficient (cm/s), Q is the water flow quantity (cm^3) over the duration time t (s), L is the length of sample (cm), H is the water head (cm), and A is the cross area of sample (cm^2).

The water permeability of pervious concrete sample used in this paper is 0.5 cm/s.

3. Failure criterion

The failure criterion used in this paper is the incubation time concept proposed by Petrov and his coauthors (Petrov and Utkin 1989, Petrov *et al*. 2010) and expressed by the formula

$$\frac{1}{\tau}\int_{t-\tau}^{t}\left[\frac{F(t')}{F_c}\right]^{\alpha}\mathrm{d}t' \leq 1 \tag{7}$$

in which, τ is the incubation time (μs), t' is the time (μs), F_c is the local static ultimate strength (kN), and α is the material sensitivity factor related to the local stress intensity. The incubation time is usually associated with the dynamic stress relaxation before the failure of specimen, and features the strain rate sensitivity. The time to failure t^* can be defined as the time at which equilibrium of Eq. (7) is reached. On the basis of the failure criterion, the incubation time equals the duration of the failure process after the force reaches to the static ultimate load on the given scale level. Therefore, this duration can be measured experimentally by static failure of the samples, and by using different valid methods, the rupturing process can be controlled.

4. Dynamic compression test results

The main objective of the dynamic compression tests is to study the effect of strain rate on the compressive behavior of pervious concrete.

To guarantee the reliability of dynamic results of quasi-brittle materials obtained from SHPB tests, the stress equilibrium should be satisfied, and the inertial effect and friction between specimen and SHPB can be neglected. In this paper, the duration of stress wave in concrete specimen is far less than the duration of impact loading. As a consequence, the force in incident bar can be assumed to be equal to that in transmitted bar, and the specimen is in a state of stress equilibrium.

The specimen can be in a stress equilibrium state when the duration time of stress wave in specimen is larger in comparison with the characteristic time of specimen t_s ($t_s=L_s/c_s$). In this test, the characteristic time of pervious concrete specimen is 7.4 μs, far less than the minimum time to failure (137 μs) of specimen.

Fig. 4 shows the dynamic stress on both ends of the pervious concrete specimen in a typical dynamic split tensile test. The dynamic stress is balanced, which is the same as the traditional SHPB test on normal concrete. The dynamic stress on one side of the specimen is the sum of the incident and reflected stress waves (P1), and the dynamic stress on the other side of the specimen is the transmitted stress wave (P2). As shown in Fig. 1, the stress on both ends of the specimen P1 (=Incident+Reflected) and P2 (=Transmitted) are in good agreement before 100 μs (i.e., P1 is equal to P2). This eliminates the global force difference and thus the inertial effects are negligible.

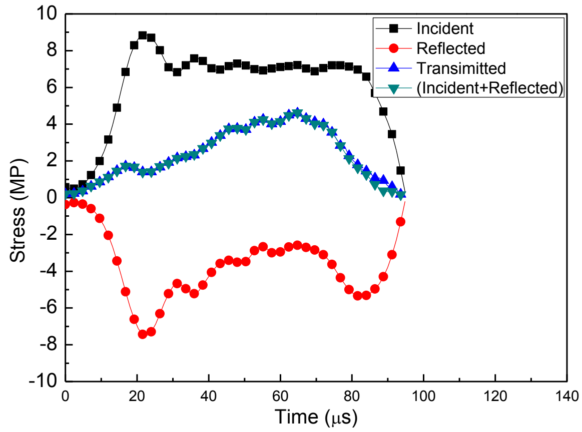

Fig. 4 Dynamic stress balance in a typical split tensile test with pulse shaping

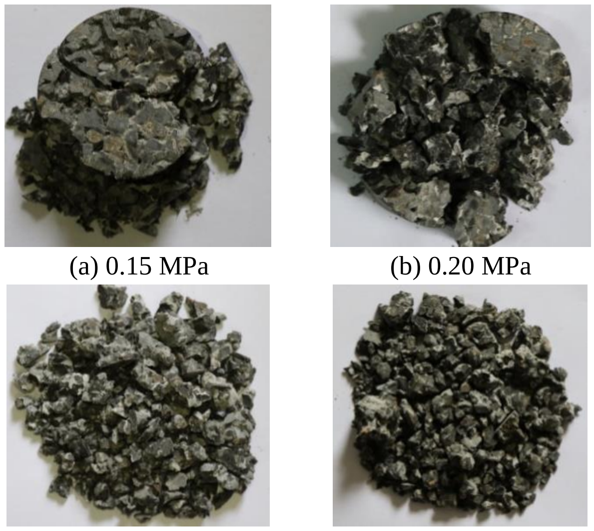

(a) 0.15 MPa (b) 0.20 MPa

(c) 0.25 MPa (d) 0.30 MPa

Fig. 5 Failure modes of specimens under various impact loading rates

Therefore, the specimen is in dynamic stress equilibrium before fracture, and the dynamic test method is reasonable for data analysis.

Furthermore, the ratio of height to diameter of concrete specimens used in this dynamic test is 0.5, so the inertial effect can be neglected (Zhang and Zhao 2014). To obtain the actual dynamic compressive stress-strain responses of pervious concrete specimens, the friction between the Hopkinson pressure bar and specimen can be reduced by grease.

Based on the above discussion, the test and data processing methods used in this paper can obtain the relationship between actual dynamic compressive strength and strain rate.

The dynamic compressive fracture modes of pervious concrete under various impacting air pressures are shown in Fig. 5. It can be seen that the dimension and numbers of fragments vary with the impacting velocity. As the impact loading rate increases, the dimension of fragments decreases while number of fragments increases.

As seen in the time history strain curve (Fig. 6), it can

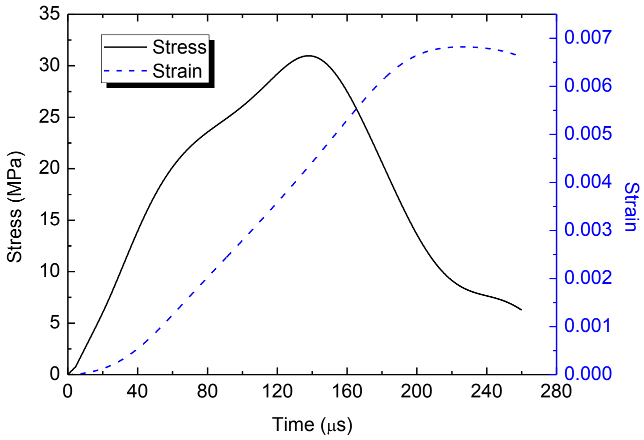

Fig. 6 The typical stress and strain time history curves of pervious concrete under dynamic compressive loading (strain rate=60/s)

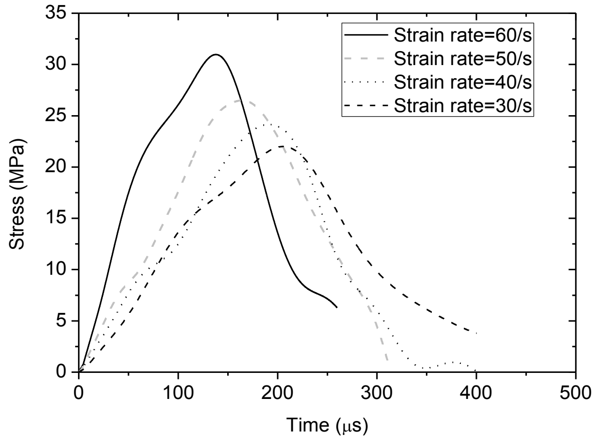

Fig. 7 The stress-time curves of pervious concrete under impact loading with various strain rates

be found that strain increases linearly with time, so the variation of strain rate can be neglected.

The time history stress curves of pervious concrete specimens under various impact loading rates are shown in Fig. 7. It indicates that the stress in specimen increases with the loading process before it reaches the critical stress σ^*at which the specimen fractures abruptly (Fig. 8). Further propagation of micro and macro cracks results in the stress relaxation and deformation extension in concrete specimen, as shown in Fig. 9. As seen in Fig. 7 and Fig. 9, it can be found that the pervious concrete is of strain rate sensitive material, namely, as strain rate increases, the time to failure decreases while the peak stress increases. Plot both the time to failure and peak stress versus time in Fig. 10, it can be seen that the stress increases linearly while the time to failure decreases linearly as increasing of strain rate.

Therefore, the dynamic compressive strength of pervious concrete related to time can be predicted on the basis of the incubation time concept. The failure criterion used in this paper can be expressed by the following formula

$$\frac{1}{\tau}\int_{t-\tau}^{t}\sigma(t')dt' \le \sigma_c^{compr} \tag{8}$$

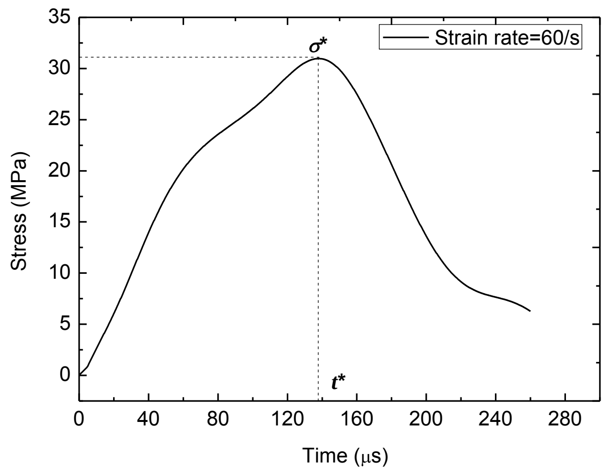

Fig. 8 The typical dynamic compressive strength and time to failure

To make the concept clear to readers, the calculation procedure is described in detail as following.

Based on the strength criterion, the strength of material can be calculated so the relationship between the strength versus strain rate can be obtained. The dynamic strength of concrete with fixed specimen dimension subjected to the specified loading condition can be calculated by using the above regression function, which avoids the tedious calculation. In this paper, the strain sensitive dynamic strength of concrete can be calculated by using the failure criterion on the basis of the incubation time concept.

It can be seen from Fig. 6 that the stress increases linearly with the loading process, which can be expressed by the following formula

$$\sigma(t) = \dot{\sigma} t H(t) = E\dot{\varepsilon} t H(t) \tag{9}$$

in which, $\dot{\sigma}$ is the stress rate (GPa/s) and $\dot{\varepsilon}$ is the strain rate (s^{-1}), $H(t)$ is the Heaviside function.

Substitute Eq. (9) to Eq. (8) and integrate it in terms of time, the ultimate dynamic compressive stress to failure can be obtained as following

$$\sigma^* = \sigma(t^*) = \begin{cases} \sigma_c^{compr} + \dot{\sigma}\tau/2 = \sigma_c^{compr} + E\dot{\varepsilon}\tau/2 & (t^* \ge \tau) \\ \sqrt{2E\dot{\varepsilon}\sigma_c^{compr}\tau} & (t^* < \tau) \end{cases} \tag{10}$$

It can be found from the above dynamic stress calculation model that the peak stress is linearly related to the strain rate when the time to failure is larger than the incubation time, which complies with the experimental results (Fig. 10). The incubation time represents the duration of the failure process after the material's stress has reached the static strength. Obviously, the dynamic strength is larger than the static strength, so the time to dynamic failure is larger than the incubation time, which meets the former half of Eq. (10). It should be noted that the above model is suitable for the stress-strain response before the peak stress.

The static compressive strength of pervious concrete can be obtained by static compression test, and it is σ_c^{compr} =12.03 MPa. The elastic modulus is obtained from the tangent modulus at the point of 40% peak stress on

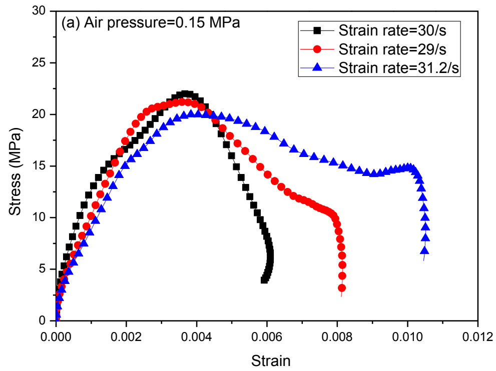

(a) Air pressure=0.15 MPa

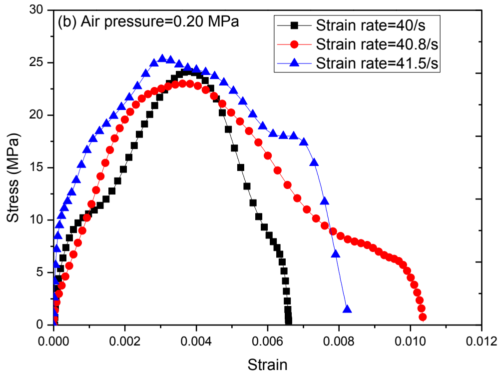

(b) Air pressure=0.20 MPa

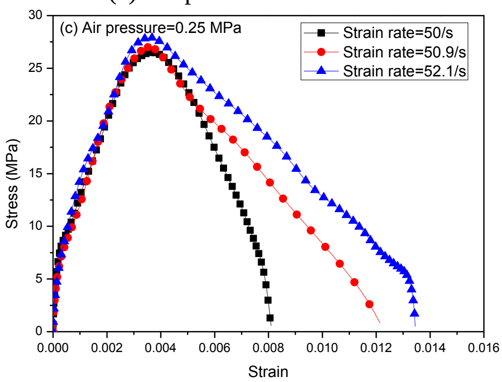

(c) Air pressure=0.25 MPa

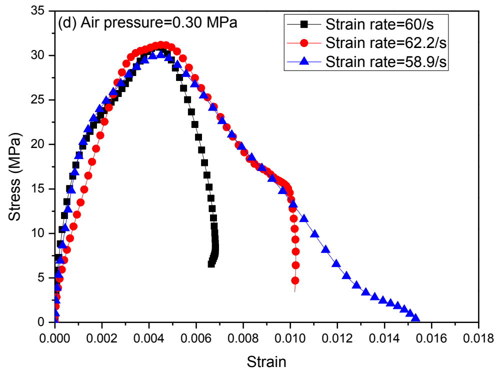

(d) Air pressure=0.30 MPa

Fig. 9 Compressive stress-strain curves of pervious concrete under various air pressures

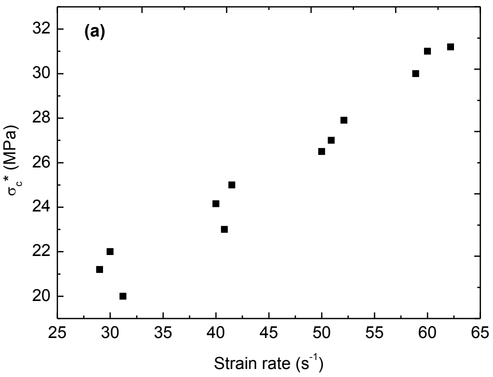

(a) The dynamic strength versus strain rate

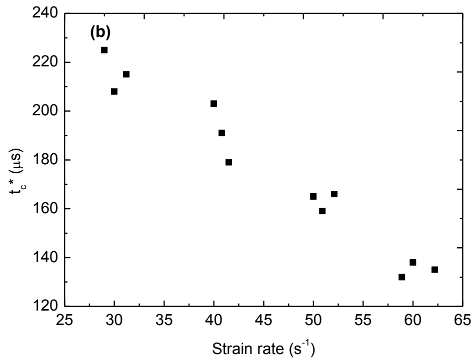

(b) The time to failure versus strain rate

Fig. 10 The dynamic compressive test results

static stress-strain curve, and it is 20 GPa. Strain rate varies with time when the concrete specimen fractures. The incubation time of the pervious concrete used in this paper can be obtained by numerical regression using the experimental results and it is 30.3 μs, which is smaller than the time to dynamic failure.

The dynamic peak stress versus strain rate is shown in Fig. 11, in which the solid symbols represent experimental data and the solid line is the fitting curve obtained by using Eq. (10) for the following set parameters: σ_c^{compr} =12.03 MPa, E=20 GPa, τ=30.3 μs. The fitting determination coefficient R^2 is 0.98. It can be found from Fig. 11 that the strain rate in a range of 20 s^{-1} to 100 s^{-1}, among which the relationship between the dynamic strength and strain rate can be obtained by using the failure criterion.

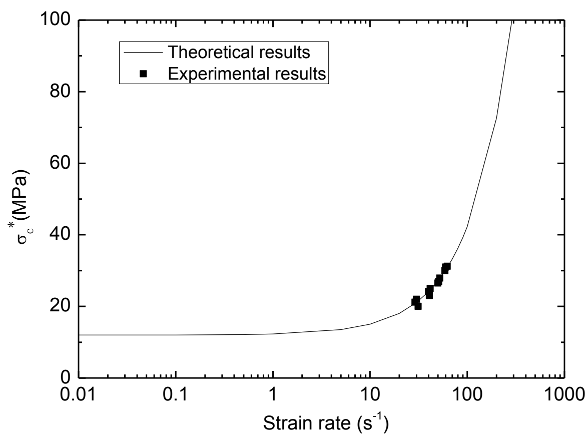

Fig. 11 The relationship between dynamic compressive strength and strain rate

(a) 0.15 MPa (b) 0.25 MPa (c) 0.35 MPa

Fig. 12 The failure mode of pervious concrete under dynamic loading

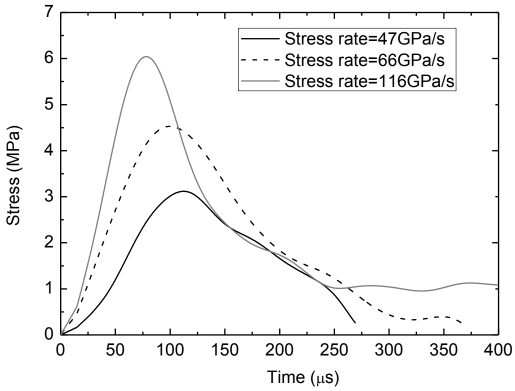

Fig. 13 The stress-time curves of pervious concrete under various loading rate

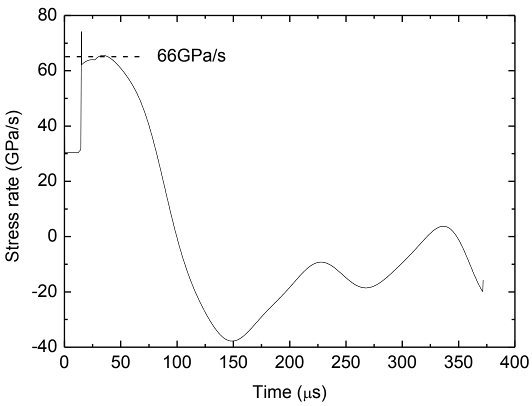

Fig. 14 The variation of strain rate with time of specimen

5. Dynamic split tensile test results

To study the effect of impact loading rate on the dynamic split tensile behavior of pervious concrete, the dynamic split tensile tests are carried out on Brazilian disc specimens by using SHPB. The dynamic split tensile test results are shown in Figs. 12-17.

As for the dynamic split tensile test, using the SHPB equipment should comply with the following two conditions. The stress distribution state in the specimen under dynamic loading should be in accordance with that under static loading. The forces acting on the incident and transmitted bars are in equilibrium. To study the stress state in the Brazilian disc specimen under dynamic loading, Chen *et al.* (2016b) demonstrated that the specimen can reach equilibrium state and be split along the diametric plane. Therefore, it can be argued that the results of the dynamic split tensile test are valid and the obtained dynamic strength enhancement can be regarded as a real material response to the stress rate.

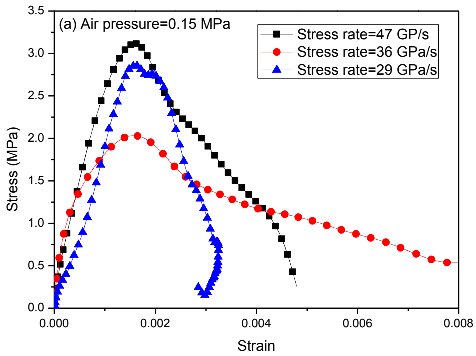

(a) Air pressure=0.15 MPa

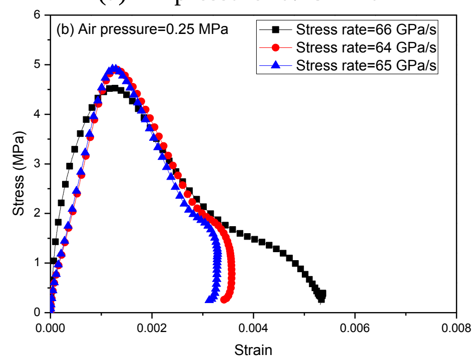

(b) Air pressure=0.25 MPa

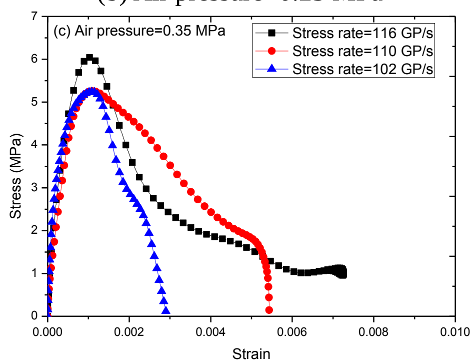

(c) Air pressure=0.35 MPa

Fig. 15 The split tensile stress-strain curves of pervious concrete under various air pressures

The fracture pattern of pervious concrete specimens under dynamic loading is shown in Fig. 12. Crack in the disc specimen initiates along the diametric plane and propagates to the platforms. It can be demonstrated that the dynamic split tensile test results are reliable. The failure mode under dynamic loading is distinct from that under static loading. Both the dynamic damaged region and the number of fragments increase with the increasing of loading rate.

The experimental stress time history curves of pervious concrete are shown in Fig. 13. It can be found that the dynamic split tensile strength increases linearly prior to peak stress in the loading process. So the stress rate during the pre-peak branch can be assumed to remain constant, and the stress rate time history curve is shown in Fig. 14. Additionally, the dynamic split tensile strength increases with the increasing of the stress rate.

Fig. 15 represents the dynamic split tensile stress-strain curves of pervious concrete under various stress rates. It can be found that the shape of stress-strain curve remains unchanged under various loading rates. And as the strain rate increases, the peak stress increases while peak strain decreases.

Figs. 16 (a) and (b) represent the variation of dynamic split tensile strength and time to failure with the stress rate, respectively. Similar to the dynamic compressive test results, as the loading rate increases, the dynamic tensile strength increases while the time to failure decreases.

According to the failure criterion, the dynamic split tensile strength can be predicted by Eq. (11).

$$\frac{1}{\tau}\int_{t-\tau}^{t}\sigma(t')dt' \leq \sigma_{c}^{\text{tensile}} \tag{11}$$

Integrate Eq. (11) in terms of time and then substitute time to failure t^* into it, the prediction model of dynamic split tensile strength can be obtained on the basis of the above failure criterion as the following formula

$$\sigma^* = \sigma(t^*) = \begin{cases} \sigma_c^{tensiler} + \dot{\sigma}\tau/2 & (t^* \geq \tau) \\ \sqrt{2E\dot{\varepsilon}\sigma_c^{compr}\tau} & (t^* < \tau) \end{cases} \tag{12}$$

The static split tensile strength of pervious concrete specimen is $\sigma_c^{\text{tensile}} = 1.66$ MPa. In Fig. 13, it can be found that the stress increases linearly with the loading process before its failure, so the strain rate can be regarded as the loading rate. The incubation time of pervious concrete under dynamic split tensile loading can be obtained by numerical regression analysis using the test data. The obtained incubation time (τ=75.5 μs) is larger than that under dynamic compressive loading.

Fig. 17 shows the relationship between the dynamic split tensile strength and strain rate. The solid symbols represent the test data and solid line represents the fitting curve in accordance with the set parameters: $\sigma_c^{\text{tensile}} = 1.66$ MPa, τ=75.5 μs).The regression determination coefficient is 0.85. It can be found that the loading rate ranges from 30 GPa/s to 120 GPa/s. The dynamic split tensile strength can be predicted on the basis of the incubation time concept.

Dynamic increase factor (DIF), which is the ratio of dynamic strength to static strength, is commonly used as an

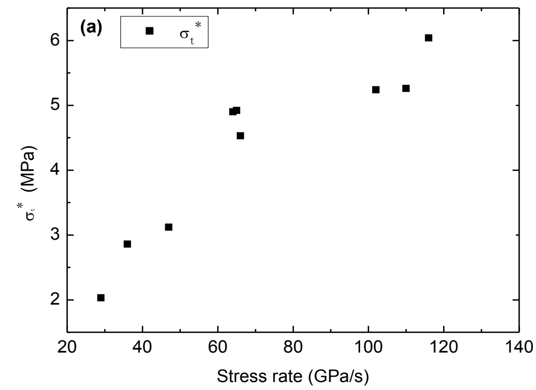

(a) The dynamic split tensile strength vs. stress rate

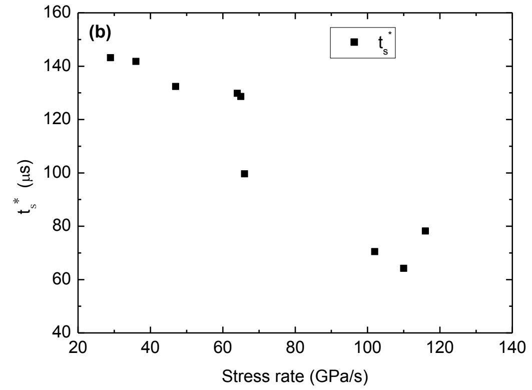

(b) The time to failure vs. stress rate

Fig. 16 The dynamic split tensile test results

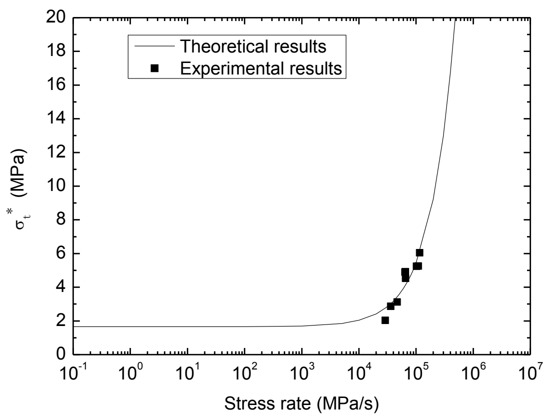

Fig. 17 The relationship between dynamic split tensile strength and stress rate

indication of the effect of strain rate of the strength of concrete materials. A bilinear relationship between DIF and the strain rate of normal concrete with a breakpoint at the strain rate of 30 s^{-1} is recommended by CEB (1993). A comparison in terms of dynamic increase factor (DIF) between the results of this test with results by Ozbek *et al*. (2013) have been provided as follows.

The recommended CEB formulas give the opportunity to see how predictable the dynamic strengths of pervious concrete are using the widely used equations. Ozbek *et al*. (2013) found that the porous concretes are strain rate dependent on materials due to the presence of cementitious material. Similar to results in literature (Ozbek *et al*. 2013),

Table 2 Experimental and calculated DIF values for pervious concretes

Mixture code	$\dot{\varepsilon}$ (s^{-1})	f_{cs} (MPa)	F_{cd} (MPa)	DIF (Experimental)	DIF (CEB model)
PRC1*	68	34.78	66.52	1.91	1.94
PRC2*	68	41.89	76.78	1.83	1.83
PRC3*	68	50.49	85.99	1.70	1.74
PRC4*	68	29.64	56.22	1.90	2.01
PRC5*	68	31.6	53.09	1.68	2.00
PRC6*	68	44.81	79.69	1.78	1.80
PRC7*	68	48.80	84.37	1.73	1.76
PRC8*	68	15.94	26.26	1.60	2.73
PRC9*	68	13.09	21.84	1.73	3.06
0.15-1	29.0	12.3	21.2	1.72	2.41
0.15-2	31.2	12.3	20.0	1.62	2.44
0.15-3	30.0	12.3	22.0	1.79	2.41
0.20-0	41.5	12.3	25.0	2.03	2.69
0.20-2	40.8	12.3	23.0	1.87	2.68
0.20-3	40.0	12.3	24.2	1.96	2.66
0.25-1	52.1	12.3	27.9	2.27	2.90
0.25-2	50.9	12.3	27.0	2.20	2.88
0.25-3	50.0	12.3	26.5	2.15	2.86
0.30-1	58.9	12.3	30.0	2.44	3.02
0.30-2	62.2	12.3	31.2	2.54	3.08
0.30-3	60.0	12.3	31.0	2.52	3.04

in this paper, the dynamic strength of pervious concrete is observed increases with the increasing of strain rate under impact loading. Test results in this paper and literature as well as predicted results by CEB (2003) are listed in Table 2 to reach better conclusions. It should be noted that, in Table 2, mixture codes with the symbol of "*" represents the test results in literature (Ozbek *et al*. 2013), and the others are test data in this paper. Ozbek *et al*. (2013) found that the experimental DIF values of the porous concrete mixtures have high static compressive strength highly consistent with the calculated DIF by using CEB model. If the concrete specimens are not sufficiently compacted, the CEB model is not valid for them. Compared to the experimental DIF values in literature, DIF in this test is large. The experimental DIF in this test is slightly smaller than the calculated DIF by using CEB model. It can be explained by that the pervious concretes are sufficiently compacted, resulting in a relatively smaller porosity. By comparing the above experimental DIF results to calculated one, it can be concluded that the calculated results using CEB model is considerably accurate for well compacted and high strength pervious concrete for the strain rate at a range of 30 to 70 s^{-1}.

6. Energy evolution theory

The specimen deforms when it is subjected to impact loading and the deformation transforms into the releasable elastic strain energy and irreversible plastic strain energy. The irreversible plastic strain leads to the internal damage, which is defined as the structural damage energy ψ_d. Defined the input energy as ψ and the elastic strain energy as ψ_e, there is

$$\psi = \psi_e + \psi_d \tag{13}$$

It is obvious that the elastic strain energy has an upper limit ψ_e^0. The entire failure process of pervious concrete under dynamic loading can be described as the following: initial equilibrium is broken when external work is acting on the specimen and then a new equilibrium can be reached as the elastic strain energy and structure failure damage increases. When the elastic strain energy increases up to ψ_e^0, specimen cannot keep balance by self-adjustment and it is in a limit equilibrium state. It fractured when the external work continued to act on the specimen. The elastic strain energy released and transformed into the kinetic energy, thermal energy and the energy in other forms.

Based on the strain equivalence principle and generalized Hook law, it can be found that the strain energy is dependent on the duration of impact loading and the stress state, and complies with the Illuin postulate (Chen *et al*. 2013). The strain is composed of elastic strain and plastic strain. The elastic strain energy can be calculated by using the stress-strain relationship in elasticity.

$$\psi_e = E\int_0^t f(\sigma, \varepsilon)\mathrm{d}t \tag{14}$$

in which, E is the equivalent elastic modulus.

If the pervious concrete is treated as an elasto-plastic material, it produces irreversible plastic strain energy under impact loading. The structure damage energy is dependent on the dissipated energy. So the damage energy can be determined by subtracting the strain energy from the total input energy. Therefore, the dynamic failure process of pervious concrete under impact loading can be described as the self-balance process of irreversible plastic energy and elastic strain energy. Namely, part of the external input work causes the damage in material and it transforms into the damage energy. The remaining external input work induces the releasable elastic strain energy, which causes material failure when it comes up to the upper limit of strain energy. The external input energy is not necessary once the failure process is triggered. The stored elastic energy and partial initial material stress energy will be released and the damage energy will accumulate when it fails.

The above three kinds of energy (incident energy W_I, reflected energy W_R and transmitted energy W_T) can be determined according to the recorded incident wave, reflected wave and transmitted wave.

$$W = \frac{A_0 C_0}{E_0}\int_0^t \sigma_*^2 \mathrm{d}t$$

(*symbolizes the corresponding stress wave) (15)

According to the relationship between the three kinds of energy, the input energy of pervious concrete specimen can be determined by subtracting the reflected and transmitted energy from the total incident energy. This input energy can be defined as the external input energy ψ acting on the pervious concrete specimen

$$\psi = W_I - W_R - W_T \tag{16}$$

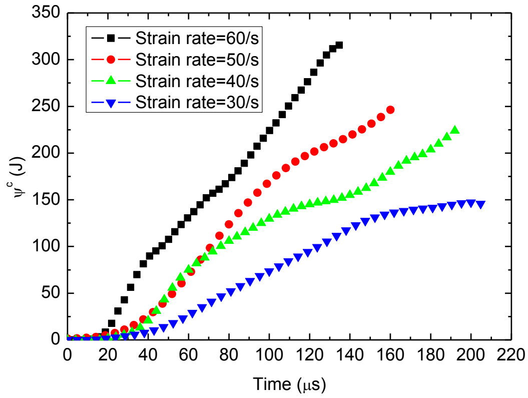

Fig. 18 The input energy of specimens under dynamic compressive loading

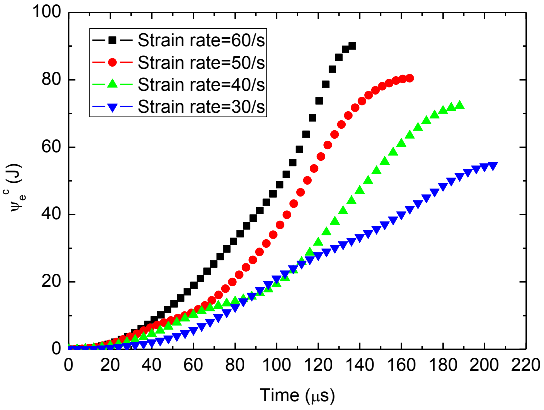

Fig. 19 The elastic strain energy of specimens under dynamic compressive loading

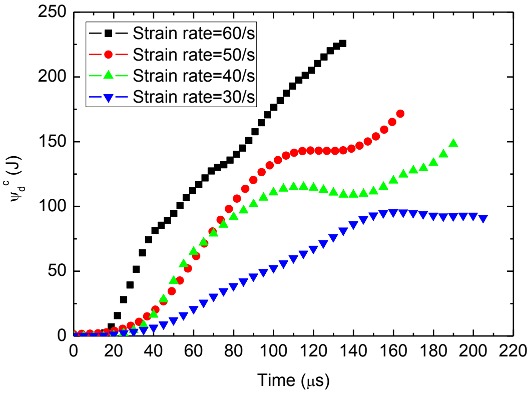

Fig. 20 The damage energy of specimens under dynamic compressive loading

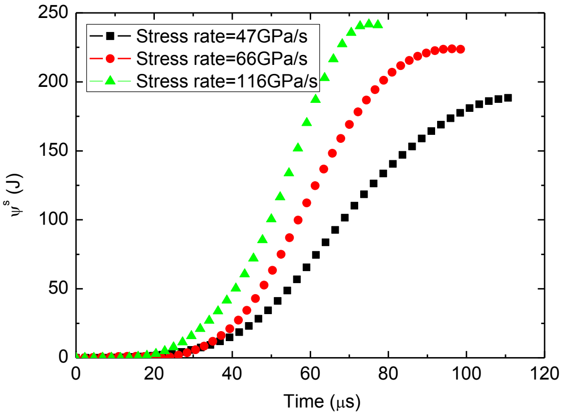

Fig. 21 The input energy of specimen under dynamic split loading

The actual energy causing damage of specimen is the input energy before the stress reaches the maximum. This is because after the point of peak stress, the dynamic failure has been triggered.

7. Energy evolution under dynamic compressive loading

The variations of input energy acting on the pervious concrete specimens with various loading rates are shown in Fig. 18. It can be found that the external input energy varies with the loading rate. The variation of accumulated input energy before 20 μs is small. After that moment, the accumulated input energy increases rapidly with the loading process. The accumulation rate of input energy and total input energy increases with the increasing of loading rate.

To further study the energy evolution of pervious concrete under dynamic compressive loading, the released elastic strain energy is analyzed on the basis of the thermodynamics principle. As shown in Fig. 19, it can be found that the variation of elastic strain energy is related to the impact loading rate. The rapid accumulation of elastic strain energy initiates later than that of total input energy. It can be explained by that the initial capillary and microcracks in pervious concrete specimen are firstly densified under dynamic compressive loading, following that the elastic strain energy increases rapidly. On the other hand, the total elastic strain energy increases with the loading rate, namely, the released energy increases with the impact loading rate, which also can be verified by the failure pattern of specimens. It can be found that the kinetic energy and thermal energy increase with the increasing of fragment number.

At the same time, the structure damage energy of pervious concrete specimen can be indirectly determined by using the external input energy and released elastic strain energy, as shown in Fig. 20. It can be found that the damage energy accumulates rapidly after 20 μs, which means that the damage of pervious concrete is a continuous accumulation process. It demonstrates that the energy causing irreversible damage in material increases with the loading rate, because the total accumulated damage energy increases with the increasing of impact loading.

8. Energy evolution under dynamic split tensile loading

The variation of external input energy acting on the pervious concrete specimens under dynamic split tensile loading is shown in Fig. 21. It indicates that the input energy increases with the increasing of stress rate. The accumulation of input energy is a slow-quick process. As

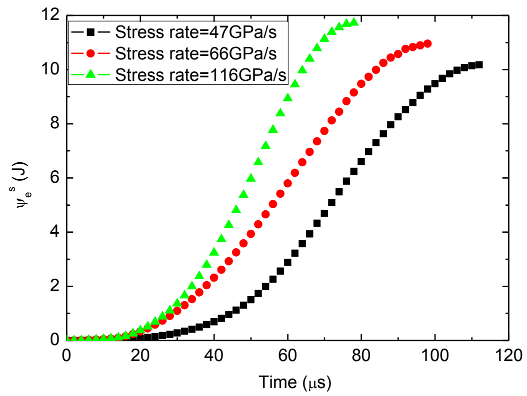

Fig. 22 The elastic strain energy of specimens under dynamic split tensile loading

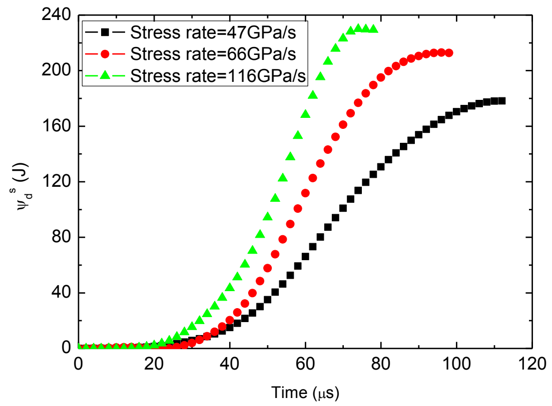

Fig. 23 The damage energy of specimens under dynamic split tensile loading

stress rate increases, the total input energy increases while the time to failure decreases.

The releasable elastic strain energy can be determined by using Eq. (14), as shown in Fig. 22. It can be found that the elastic strain energy is dependent on the stress rate. The total accumulated elastic strain energy increases with the increasing of impact loading rate. Namely, the energy released from the concrete specimen after it fractures increases with the increasing of impact loading rate. The failure mode indicates that the number of fragments increases with the increasing of loading rate.

The damage energy of pervious concrete specimen under dynamic split tensile loading can also be determined, as shown in Fig. 23. It demonstrated that the accumulation of damage energy is a continuous process, and the damage energy increases rapidly after the duration of 25 μs. The total damage energy increases with the increasing of loading rate.

9. Fractal characteristics of pervious concrete fragmentation

Before the dynamic compressive test, labeled and weighed the specimens. After the dynamic test, collect the fragments and classify them by using the sieve with diameter of 0.075, 0.15, 0.3, 0.6, 1.25, 2.5, 5.0, and 10.0 mm.

Fractal is an available method to describe the irregular phenomena. Fractal dimension is an important character to indicate the fractal (Zhou *et al*. 2006).

The damage evolution of pervious concrete material is a complex process, which depends on the composition of material, loading condition and loading rate *et al*. Some researchers have devoted themselves to studying the distribution of rock fragmentations under impact loading and have proposed some classical size distribution models (Nagahama 1993). By comparing the classical size distribution models of fragments, a unified expression to describe it has been obtained as following

$$\frac{m(r)}{M}=\left(\frac{r}{r_m}\right)^b \tag{17}$$

in which, m (g) is the sieving mass corresponding to the characteristic size r (mm), M is the total mass of fragments, r_m represent the maximum size of the fragmentations, and b is the regression coefficient.

Then, there is

$$dm \propto r^{b-1}dr \tag{18}$$

Based on the relationship between the size of fragmentations and corresponding passing mass, there is the following formula

$$dm \propto r^3 dN \tag{19}$$

Therefore, the fractal dimension can be determined based on Eq. (20)

$$D=3-b \tag{20}$$

In this way, the fractal dimension of pervious concrete fragmentations under various impact loading rates can be determined.

The size distributions of pervious concrete fragmentations under four various impacting pressures are shown in Fig. 24, in which the solid lines represent the fitting curves. To distinct the size distribution of fragmentations under different loading rates, only one of the distribution curves of fragmentations under the same pressure is plotted in Fig. 24, and the corresponding parameters are listed in Table 3.

Table 3 The calculated fractal dimensions of pervious concrete fragments

Air pressure (MPa)	$\dot{\varepsilon}$ (s^{-1})	b	D	R^2
0.15	30.0	1.896	1.104	0.96
0.15	29.2	1.719	1.281	0.94
0.15	31.2	1.681	1.319	0.93
0.20	40.0	1.608	1.392	0.93
0.20	41.5	1.578	1.422	0.93
0.20	40.8	1.577	1.423	0.93
0.25	50.0	1.500	1.500	0.92
0.25	52.1	1.469	1.531	0.98
0.25	50.9	1.445	1.555	0.95
0.30	58.9	1.38	1.62	0.95
0.30	62.2	1.325	1.675	0.93
0.30	60.0	1.219	1.781	0.96

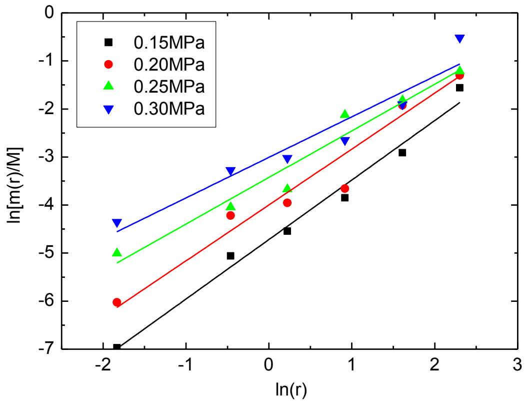

Fig. 24 The relationship between particle size and sieving percentage of particles

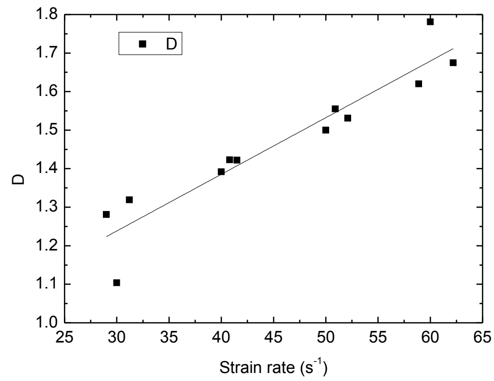

Fig. 25 The relationship between fractal dimension and strain rate of pervious concrete under dynamic compressive loading

It can be found that, by using the above proposed model, the simulated size distribution curves of fragments fit well with the test results, and all the determination coefficient are larger than 0.92. So the calculated fractal dimension is reliable. The fractal dimensions of pervious concrete specimens in this paper range from 1.1 to 1.8. It can be found that the fractal dimension increases with the loading rate as shown in Fig. 25. It demonstrated that, as the strain rate increases, the size of fragments decreases while the number of the fragments increases. The fractal dimension and impact loading rate satisfy the following relationship

$$D = 0.015\dot{\varepsilon} + 0.798 \qquad R^2 = 0.88 \tag{21}$$

in which, D represents the fractal dimension, and $\dot{\varepsilon}$ is the strain rate (s^{-1}).

10. Conclusions

The dynamic properties of pervious concrete under dynamic compressive and split tensile loading were studied by using split Hopkinson pressure bar equipment. The dynamic failure of pervious concrete material was analyzed by failure criterion on the basis of incubation time concept, which can be used to predict the dynamic strength and time to failure. Additionally, the energy evolution of pervious concrete under dynamic loading was analyzed. The energy evolution characterizes the fracture process of materials like concrete. Finally, the effect of strain rate on fragmentation of pervious concrete under impact loading was also investigated on the basis of the fractal theory. The main conclusions can be drawn as follows:

• It is argued that the pervious concrete is strain rate sensitive. In the range of strain rate in this test, the dynamic strength increases linearly while the time to failure approximately decreases linearly with the increasing of strain rate.

• The dynamic compressive and split tensile strength can be accurately predicted on the basis of the failure criterion. It indicates that the calculated peak stress is linearly related to the strain rate, which is in accordance with the experimental result.

• When it comes to the energy evolution of pervious concrete, it can be found that the accumulated rate of input energy and the corresponding total input energy increases with the increasing of impact loading. The rapid accumulation of elastic strain energy is observed to occur lately than that of input energy. The total damage energy is found to increase with the increasing of impact loading, which presents that the energy producing irreversible damage is larger.

• The fragment pattern of pervious concrete under dynamic loading is also investigated on the basis of the fractal theory. It demonstrates that the fractal dimension increases with the increasing of impact loading rate, which means that, as the loading rate increases, the size of fragments decreases while the amount of fragments increases.

Acknowledgements

This research is based upon work supported by the National Natural Science Foundation of China (Grant No. 51779085), Youth Elite Scientists Sponsorship Program by CAST (2017QNRC001), Investigation on Slope Protection Technology of Eco High Performance Concrete (20188058216) and the Open Foundation of State Key Laboratory of Hydrology-Water Resources and Hydraulic Engineering (Grant No. 2017491711).

References

ACI 522R (2010), Report on Pervious Concrete, ACI 522R-10, American Concrete Institute.

Brara, A. and Klepaczko, J.R. (2006), "Experimental characterization of concrete in dynamic tension", *Mech. Mater.*, **38**(3), 253-267.

Cadoni, E., Asprone, D. and Prota, A. (2007), "High strain rate testing of concrete and steel for the assessment of the Tenza Bridge under blast loading", *Fracture Mechanics of Concrete and Concrete Structures- New Tends in Fracture Mechanics of Concrete, Taylor & Francis Group*, London.

Chen, T. *et al*. (2013), "Research on rock energy evolution in the process of impact compression failure", *Chin. J. Underg. Space Eng.*, **9**(s1), 1477-1482. (in Chinese)

Chen, X., Ge, L. and Yuan, H. (2016a), "Effect of pre-static loading on dynamic tensile strength of concrete under high strain rates", *ASCE J. Mater. Civil Eng.*, **28**(12), 06016018.

Chen, X., Ge, L., Chen, C. and Xu, L. (2016b), "Influence of initial static splitting tensile loading on dynamic compressive strength of concrete cores under high strain rates", *ASCE J. Perform. Constr. Facil.*, **30**(6), 06016002.

Chen, X., Ge, L., Zhou, J. and Wu, S. (2017), "Dynamic Brazilian test of concrete using split Hopkinson pressure bar", *Mater. Struct*., **50**(1), 1-15.

Chen, X.D., Wu, S.X. and Zhou, J.K. (2014), "Experimental study on dynamic tensile strength of cement mortar using split Hopkinson pressure bar technique", *ASCE J. Mater. Civil Eng.*, **26**(6), 04014005.

Chen, X.D., Wu, S.X. and Zhou, J.K. (2015), "Compressive strength of concrete cores under high strain rates", *J. Perform. Constr. Facil*., **29**(1), 06014005.

Comité Euro-International du Béton (1993), CEB-FIP Model Code 1990, Redwood Books, Trowbridge, Wiltshire, UK.

De Andrade Silva, F., Butler, M., Mechtcherine, V., Zhu, D. and Mobasher, B. (2011), "Strain rate effects on the tensile behavior of textile-reinforced concrete under static and dynamic loading", *Mater. Sci. Eng. A*, **528**(3), 1727-1734.

Erzar, B. and Forquin, P. (2010), "An experimental method to determine the tensile strength of concrete under high rates of strain", *Exp. Mech*., **50**(7), 941-955.

Fu, Q., Xie, Y., Long, G., Niu, D., Song, H. and Liu, X. (2017), "Impact characterization and modelling of cement and asphalt mortar based on SHPB experiments", *Int. J. Impact Eng.*, **106**, 44-52.

Hao, H., Hao, Y. and Li, Z.X. (2009), "A numerical study of factors influencing high-speed impact tests of concrete material properties", *Keynote in Proceedings of the 8th International Conference on Shock and Impact Loads on Structures*, CI-Premier Pte Ltd., Adelaide.

Joshaghani, A., Ramezanianpour, A.A., Ataei, O. and Golroo, A. (2015), "Optimizing pervious concrete pavement mixture design by using the Taguchi method", *Constr. Build. Mater.*, **101**, 317-325.

Kuo, W.T., Liu, C.C. and Su, D.S. (2013), "Use of washed municipal solid waste incinerator bottom ash in pervious concrete", *Cement Concrete Compos.*, **37**, 328-335.

Li, J.C., Li, N.N., Li, H.B. and Zhao, J. (2017), "An SHPB test study on wave propagation across rock masses with different contact area ratios of joint", *Int. J. Impact Eng.*, **105**, 109-116.

Li, L. and Aubertin, M. (2003), "A general relationship between porosity and uniaxial strength of engineering materials", *Can. J. Civil Eng.*, **30**(4), 644-658.

Lian, C. and Zhuge, Y. (2010), "Optimum mix design of enhanced permeable concrete-an experimental investigation", *Constr. Build. Mater.*, **24**(12), 2664-2671.

Lian, C., Zhuge, Y. and Beecham, S. (2011), "The relationship between porosity and strength for porous concrete", *Constr. Build. Mater.*, **25**(11), 4294-4298.

Monters, F. (2006), "Pervious concrete: characterization of fundamental properties and simulation of microstructure", PhD Dissertation, University of south Carolina, USA.

Nagahama, H. (1993), "Fractal fragment size distribution for brittle rocks", *Int. J. Rock Mech. Min. Sci. Geomech. Abs.*, **30**(4), 469-471.

Novo, A.V., Bayon, J.R., Castro-Fresno, D. and Rodriguez-Hernandez, J. (2013), "Temperature performance of different pervious pavements: Rainwater harvesting for energy recovery purposes", *Water Resour. Manage.*, **27**(15), 5003-5016.

Ozbek, A.S.A., Weerheijm, J., Schlangen, E. and van Breugel, K. (2013), "Dynamic behavior of porous concretes under drop weight impact testing", *Cement Concrete Compos.*, **39**, 1-11.

Petrov, Y.V. and Utkin, A.A. (1989), "Dependence of the dynamic strength on loading rate", *Mater. Sci.*, **25**(2), 153-156.

Petrov, Y.V., Smirnov, I.V. and Utkin, A.A. (2010), "Effects of strain-rate strength dependence in nanosecond load duration range", *Mech. Solid.*, **45**(3), 476-484.

Rehder, B., Banh, K. and Neithalath, N. (2014), "Fracture behavior of pervious concretes: the effects of pore structure and fibers", *Eng. Fract. Mech.*, **118**, 1-16.

Rossi, P., van Mier, J.G.M., Toutlemonde, F., Le Maou, F. and Fabrice Boulay, C. (1994), "Effect of loading rate on the strength of concrete subjected to uniaxial tension", *Mater. Struct.*, **27**(5), 260-264.

Shen, W., Shan, L., Zhang, T., Ma, H., Cai, Z. and Shi, H. (2013), "Investigation on polymer-rubber aggregate modified porous concrete", *Constr. Build. Mater.*, **38**, 667-674.

Sumanasooriya, M.S. and Neithalath, N. (2011), "Pore structure features of pervious concretes proportioned for desired porosities and their performance prediction", *Cement Concrete Compos.*, **33**(8), 778-787.

Tian, Z. *et al*. (2016), "Effect of strain rate and moisture content on dynamic mechanical behaviours of mortar", *Int. J. Pavement Eng.*, **17**(9), 789-798.

Torres, A., Hu, J and Ramos, A. (2015), "The effect of the cementitious paste thickness on the performance of pervious concrete", *Constr. Build. Mater.*, **95**, 850-859.

Volder, A., Watson, T. and Viswanathan, B. (2009), "Potential use of pervious concrete for maintaining existing mature trees during and after urban development", *Urban Forest Urban Green.*, **8**(4), 249-256.

Weerheijm J. (2016), "Design and analyses of porous concrete for safety applications", PhD Dissertation, Delft University of Technology, Delft.

Xiao, S.Y., Li, J.B. and Mo, Y.L. (2017), "Dynamic bending behaviours of RC beams under monotonic loading with variable rates", *Comput. Concrete*, **20**(3), 349-360

Yan, D. and Lin, G. (2006), "Dynamic properties of concrete in direct tension", *Cement Concrete Res.*, **36**(7), 1371-1378.

Zhang, Q.B. and Zhao, J. (2014), "A review of dynamic experimental techniques and mechanical behaviour of rock materials", *Rock Mech. Rock Eng.*, **47**(4), 1411-1478.

Zhong, R. and Wille, K. (2016), "Linking pore system characteristics to the compressive behavior of pervious concrete", *Cement Concrete Compos.*, **70**, 130-138.

Zhou, Z.L., Li, X.B., Zuo, Y.J. and Hong, L. (2006), "Fractal characteristics of rock fragmentation at strain rate of 100-102 s-1", *J. Central South Univ. Technol.*, **13**(3), 290-294.

Zhu, D., Peled, A. and Mobasher, B. (2011), "Dynamic tensile testing of fabric-cement composites", *Constr. Build. Mater.*, **25**(1), 385-395.

Zielinski, A.J., Reinhardt, H.W. and Kormeling, H.A. (1981), "Experiments on concrete under uniaxial impact loading", *Mater. Struct.*, **14**(2), 103-112.

CC